



# BIFURCATION ANALYSIS OF ITERATIVE IMAGE RECONSTRUCTION METHOD FOR COMPUTED TOMOGRAPHY

TETSUYA YOSHINAGA\*, YOSHIHIRO IMAKURA<sup>†</sup>,  
KEN'ICHI FUJIMOTO\* and TETSUSHI UETA<sup>†</sup>

*\*Department of Radiologic Science and Engineering,  
Faculty of Medicine, The University of Tokushima,  
Tokushima 770-8509, Japan*

*<sup>†</sup>Graduate School of Engineering,  
The University of Tokushima,  
Tokushima 770-8506, Japan*

Received March 9, 2007; Revised April 20, 2007

Of the iterative image reconstruction algorithms for computed tomography (CT), the power multiplicative algebraic reconstruction technique (PMART) is known to have good properties for speeding convergence and maximizing entropy. We analyze here bifurcations of fixed and periodic points that correspond to reconstructed images observed using PMART with an image made of multiple pixels and we investigate an extended PMART, which is a dynamical class for accelerating convergence. The convergence process for the state in the neighborhood of the true reconstructed image can be reduced to the property of a fixed point observed in the dynamical system. To investigate the speed of convergence, we present a computational method of obtaining parameter sets in which the given real or absolute values of the characteristic multiplier are equal. The advantage of the extended PMART is verified by comparing it with the standard multiplicative algebraic reconstruction technique (MART) using numerical experiments.

**Keywords:** Computed tomography; iterative image reconstruction; bifurcation; discrete dynamical system; PMART.

## 1. Introduction

Iterative reconstruction [Gordon *et al.*, 1970; Kak & Slaney, 1987; Stark, 1987; Shepp & Vardi, 1982] is a well-known method of reconstructing computed tomography (CT) images, and it has advantages over the filtered back-projection procedure, which is commonly used for CT reconstruction in medical practices, in reducing artifacts. Because of the high quality of these reconstructions, a lot of research [Gordon & Herman, 1974; Snyder *et al.*, 1992; Herman & Meyer, 1993; Wang *et al.*, 1996; Mueller *et al.*, 1999; Man *et al.*, 2001; Byrne, 2004] has been done on improving the iterative deblurring

procedures. Of the iterative reconstruction algorithms, the power multiplicative algebraic reconstruction technique (PMART) [Badea & Gordon, 2004; Byrne, 2004] has good properties for maximizing entropy; however, it requires a large number of iterations to obtain the final reconstructed image for large data sets.

The final reconstructed image obtained by applying an iterative reconstruction algorithm for appropriate initial pixel values corresponds to a fixed or periodic point observed in the dynamical system describing the iterative reconstruction technique. An analysis of bifurcation is useful for

investigating the stability of fixed points and in designing system parameters. In this paper, we calculate a two-parameter bifurcation diagram for PMART with an image obtained with  $2 \times 2$  pixels. Our bifurcation analysis of PMART with multiple pixels, which was applied for the first time, enabled us to observe various kinds of nonlinear phenomena such as the coexistence of a false image, the transition of stability of fixed points, and the generation of a two-periodic point, by changing one of the system parameters. The results also suggest appropriate parameter regions and phantom-image values within the PMART can operate normally.

To improve the speed of convergence, we propose an extended PMART, which is a dynamical class that includes the multiplicative algebraic reconstruction technique (MART) as well as PMART. The process of convergence for iterative points in the neighborhood of a reconstructed image can be reduced to the property of the characteristic multiplier of a stable fixed point observed in the dynamical system. To investigate the behavior of convergence, we present a computational method of obtaining parameter sets in which the given real or absolute values of the characteristic multiplier are equal. The advantage of the extended PMART is verified by comparing it with the standard MART using numerical experiments.

## 2. Method of Analysis

All iterative reconstruction procedures treated in this paper are considered to be nonlinear dynamical systems. The theoretical background and methods of analysis using qualitative bifurcation theory are summarized in this section.

### 2.1. Fixed point and its bifurcation

Let us consider a discrete dynamical system, or equivalently, a map defined by

$$T_\nu : R^n \rightarrow R^n; \quad x^{(k)} \mapsto x^{(k+1)} = T_\nu(x^{(k)}), \quad (1)$$

where  $x \in R^n$  denotes the state of discrete time  $k = 1, 2, \dots$ , and  $\nu \in R$  indicates a system parameter. The point,  $x^*$ , satisfying

$$x^* - T_\nu^m(x^*) = 0 \quad (2)$$

becomes a fixed ( $m = 1$ ) or an  $m$ -periodic ( $m > 1$ ) point of  $T_\nu$ . Let  $x^*$  be a periodic point of  $T_\nu$ ; then the characteristic equation for periodic point  $x^*$  is defined by

$$\chi(x^*, \nu, \mu) = \det(\mu E - DT_\nu^m(x^*)) = 0, \quad (3)$$

where  $E$  is the  $n \times n$  identity matrix, and  $DT_\nu^m$  denotes the derivative of  $T_\nu^m$ . We say  $x^*$  is hyperbolic if all the absolute values of the eigenvalues of  $DT_\nu^m$  differ from unity. We will only consider the properties of a fixed point of  $T_\nu$  in the following. A similar argument can be applied to the periodic point of  $T_\nu$ .

Now let us consider a topological classification of a hyperbolic fixed point. Let  $x^*$  be a hyperbolic fixed point and  $E^u$  be the intersection of  $R^n$  and the direct sum of the generalized eigenspaces of  $DT_\nu(x^*)$  corresponding to the eigenvalues,  $\mu$ , such that  $|\mu| > 1$ . Let  $L^u = DT_\nu(x^*)|_{E^u}$ . Then, the topological type of a hyperbolic fixed point is determined by  $\dim E^u$  and the orientation-preserving or reversing property of  $L^u$ .

Let us define four types of hyperbolic fixed points [Kawakami, 1984]:

- (1) *PD*-type if  $\dim E^u$  is even and  $\det L^u > 0$ ,
- (2) *ND*-type if  $\dim E^u$  is odd and  $\det L^u > 0$ ,
- (3) *PI*-type if  $\dim E^u$  is even and  $\det L^u < 0$ , and
- (4) *NI*-type if  $\dim E^u$  is odd and  $\det L^u < 0$ .

From the definitions, at a *PD*- or an *ND*-type of fixed point  $x^*$ ,  $L^u$  is orientation-preserving mapping, whereas at a *PI*- or an *NI*-type of fixed point  $x^*$ ,  $T_\nu$  is orientation-reversing mapping. If  $E^u$  is an empty set, we identify  $x^*$  as a *PD*-type. We use the symbol  ${}_\ell M^m$  for a hyperbolic periodic point, where  $M$  denotes one of the *PD*, *ND*, *PI* or *NI* types,  $\ell$  indicates the number of characteristic multipliers outside the unit circle in the complex plane, and  $m$  indicates an  $m$ -periodic point, which will be omitted for  $m = 1$ .

Bifurcation occurs when the topological type of a fixed point is changed by varying a system parameter. The generic codimension-one bifurcations are: tangent, period-doubling and Neimark–Sacker bifurcations. These bifurcations are observed when hyperbolicity is destroyed, which corresponds to the critical distribution of characteristic multiplier  $\mu$  such that  $\mu = +1$  for tangent bifurcation,  $\mu = -1$  for period-doubling bifurcation, and  $\mu = e^{j\theta}$  for Neimark–Sacker bifurcation, where  $j = \sqrt{-1}$ .

### 2.2. Equal characteristic multiplier

The behavior of convergence in the neighborhood of a stable fixed point is governed by the characteristic multipliers or eigenvalues of the derivative of  $T_\nu$  with respect to the fixed point. To investigate a parameter region in which the system has a locally

faster convergence speed, we propose a method of calculating a set of both a parameter and a fixed point with a given equal real or absolute value for the characteristic multiplier.

### 2.2.1. With a real characteristic multiplier

When the specified real characteristic multiplier is denoted by  $\mu^*$ , the condition is given by

$$\chi(x, \nu, \mu^*) = \det(\mu^* E - DT_\nu(x)) = 0 \quad (4)$$

Therefore, we can obtain unknown set  $(x, \nu) \in R^n \times R$  by solving the fixed point equation (2) and the condition of Eq. (4) simultaneously.

### 2.2.2. With a complex characteristic multiplier

When the specified absolute value of the characteristic multiplier is denoted by  $\rho^*$ , the condition is given by

$$\chi(x, \nu, \rho^* e^{j\theta}) = \det(\rho^* e^{j\theta} E - DT_\nu(x)) = 0, \quad (5)$$

where  $j$  is the imaginary unit, and  $\theta$  is the argument of a complex characteristic multiplier. To obtain the unknown set  $(x, \nu, \theta) \in R^n \times R \times R$ , we solve simultaneous equations consisting of the fixed point equation (2) and the following two equations:

$$\begin{aligned} \chi_1(x, \nu, \rho^* e^{j\theta}) &= \Re[\det(\rho^* e^{j\theta} E - DT_\nu(x))] = 0 \quad \text{and} \\ \chi_2(x, \nu, \rho^* e^{j\theta}) &= \Im[\det(\rho^* e^{j\theta} E - DT_\nu(x))] = 0, \end{aligned} \quad (6)$$

where  $\Re$  and  $\Im$  denote the real and imaginary parts, respectively.

For the numerical determination of the above contour sets, we have used Newton's method. The Jacobian matrix of the set of equations is derived from the first and second derivatives of map  $T_\nu$ . This procedure is an extension of Kawakami's method [Kawakami, 1984] of finding bifurcation parameters. Note that tangent and period-doubling bifurcations (resp. the Neimark–Sacker bifurcation) can be obtained by using the same method for  $\mu^* = 1$  (resp.  $\rho^* = 1$ ) in Eq. (4) (resp. Eq. (6)).

## 3. Systems

### 3.1. Definition and analysis of PMART

Consider a  $J$ -dimensional discrete dynamical system  $x^{(k+1)} = f(x^{(k)})$ ,  $k = 1, 2, \dots$ , or a map

defined by

$$f : R^J \rightarrow R^J; \quad x \mapsto f(x), \quad (7)$$

where  $x^{(k)}$  and  $x = (x_1, x_2, \dots, x_J)'$  are state vectors in  $R^J$ , each of which corresponds to the successive estimate of the reconstructed value of an iterative algorithm in image reconstruction. PMART [Badea & Gordon, 2004; Byrne, 2004] can be written in mapping form with the following elements  $f_j$ s for  $j = 1, 2, \dots, J$ :  $f_j = f_j^I \circ f_j^{I-1} \circ \dots \circ f_j^1$  with the  $i$ th submap

$$f_j^i = x_j \left( \frac{q^i}{p^i x} \right)^{\gamma p_j^i}, \quad (8)$$

where  $p^i = (p_1^i, p_2^i, \dots, p_J^i)$  is the normalized projection operator applied on the  $x$  image,  $q^i$  and  $p^i x$  are the respective projection and reprojection values corresponding to the  $i$ th ray for  $i = 1, 2, \dots, I$ , and  $\gamma$  is a positive real parameter.

The following theoretical result gives an extension to the arbitrary numbers of both  $J$  and  $I$  of the convergence/divergence properties discussed in [Badea & Gordon, 2004] for the scalar case.

The derivative of  $f$  with respect to  $x$  is given by

$$\frac{\partial f}{\partial x} = \frac{\partial f^I}{\partial x} \frac{\partial f^{I-1}}{\partial x} \dots \frac{\partial f^1}{\partial x},$$

and the derivative of each submap  $f^i$  can be obtained by

$$\begin{aligned} \frac{\partial f^i}{\partial x} &= \text{diag}_j \left\{ \left( \frac{q^i}{p^i x} \right)^{\gamma p_j^i} \right\} \\ &\quad \times \left( E - \frac{\gamma}{p^i x} \text{diag}_j \{x_j\} \cdot p^i \cdot p^{i'} \right) \end{aligned}$$

for  $i = 1, 2, \dots, I$ , where  $E$  denotes the  $J \times J$  identity matrix. By direct calculation, we can see that the eigenvalues of the Jacobian  $\partial f^i / \partial x$  ( $i = 1, 2, \dots, I$ ) at the fixed point, corresponding to the exact image of  $f$  are

$$\underbrace{1, 1, \dots, 1}_{J-1} \quad \text{and} \quad 1 - \gamma.$$

Therefore, when the value of  $\gamma$  is 2 or the critical power [Badea & Gordon, 2004], the absolute values of the determinants of the derivatives for map  $f$  as well as each submap  $f^i$  at the fixed point are all 1, and every characteristic multiplier of the fixed point is located on the unit circle in the complex plane. Moreover, the fixed point is stable when the value of  $\gamma$  is less than 2, and unstable when the value is greater than 2.

### 3.2. Extended PMART

Let us now consider a dynamical system defined by

$$g: R^J \rightarrow R^J; \quad x \mapsto (1 - \lambda)x + \lambda f(x), \quad (9)$$

where  $f$  denotes the map of PMART in Eq. (7) with Eq. (8), and  $\lambda \in R$  is a weight parameter. Note that the expression in Eq. (9) includes the algorithms of MART when  $(\lambda, \gamma) = (1, 1)$ , and PMART when  $\lambda = 1$ . Also note that the extended PMART with  $\gamma = 1$  and  $\lambda \leq 1$  describes RMART (rescaled-MART) [Byrne, 2004], in which the convergence of non-negative solutions to a unique stable fixed point is guaranteed. Taking advantage of the nonlinear dynamics of the weighted averaging-PMART with wide parameter ranges of  $\gamma$  and  $\lambda$ , we demonstrate that it contributes to the acceleration of convergence.

As theoretically discussed in the previous subsection, when  $J \geq 2$ , the dynamical system  $f$  at  $\gamma = 2$  has a nonhyperbolic fixed point whose characteristic multipliers are generally complex and on the unit circle in the complex plane. Then, by decreasing  $\gamma$  through the degenerate bifurcation value, an invariant closed curve (ICC) generated around the fixed point in the state space disappears with changing  $\dim E^u$  from  $J$  to 0, and the iterative points converge to the stable fixed point along the center manifold that is qualitatively equivalent to the spiral. Due to the attracting spiral behavior,  $g(x)$ , which is considered to be a weighted average of point  $x$  and the next iterate  $f(x)$ , is expected to obtain a better estimate than  $f(x)$  for an appropriate value of the weight parameter,  $\lambda$ .

## 4. Experimental Results

To illustrate the efficiency of the proposed iterative algorithm and the computational method, we use

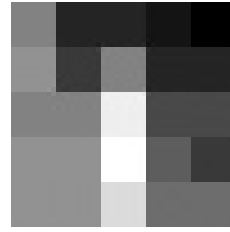


Fig. 1. Phantom image of  $5 \times 5$  pixels.

two examples: (i) the first image is made of four pixels and six projection rays with the projection operators  $p^1 = (1, 1, 0, 0)$ ,  $p^2 = (0, 0, 1, 1)$ ,  $p^3 = (1, 0, 0, 1)$ ,  $p^4 = (0, 1, 0, 1)$ ,  $p^5 = (1, 0, 1, 0)$ , and  $p^6 = (0, 1, 1, 0)$ , and the phantom image  $x^* = (5, 6, 7, 2)'$ . (ii) The second image is made of  $5 \times 5$  pixels and 56 projection rays with the phantom image shown in Fig. 1.

Figure 2 shows an ICC forming a torus observed in map  $f$  for the first example ( $J = 4$ ) with  $\gamma = 2$ , consisting of 100,000 iterated points. The characteristic multipliers of the fixed point satisfy the condition of the double Neimark–Sacker bifurcation as a codimension-two bifurcation.

### 4.1. Bifurcation analysis of PMART

Let us consider a two-parameter bifurcation problem with the PMART in Eq. (7) with the parameter settings of example (i). The first bifurcation parameter is the power exponent,  $\gamma$ , and the second is the first element of the phantom image,  $x_1^*$ .

Figure 3 is a diagram of bifurcations denoted by thick solid, thin solid and dashed lines with the symbols  $T^m$ ,  $P_\ell$ , and  $NS^m$  for tangent, period-doubling and Neimark–Sacker bifurcations. The superscript number  $m$  indicates an  $m$ -periodic point, and the subscript  $\ell$  denotes the number to distinguish

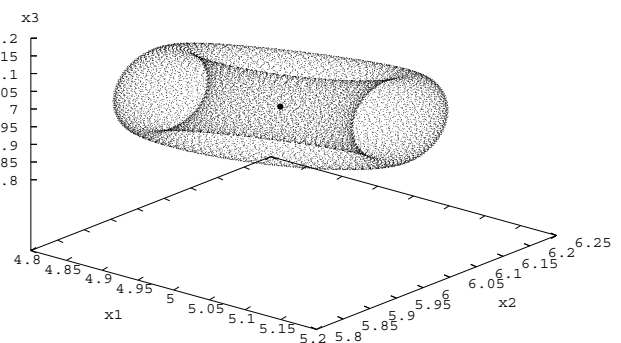
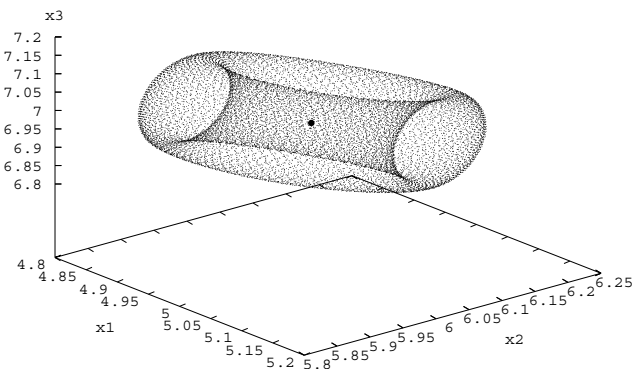


Fig. 2. Perspective figure of an ICC observed in  $f$  with  $J = 4$  and  $\gamma = 2$ . The fixed point is located at the circled point at the center of iterated points.



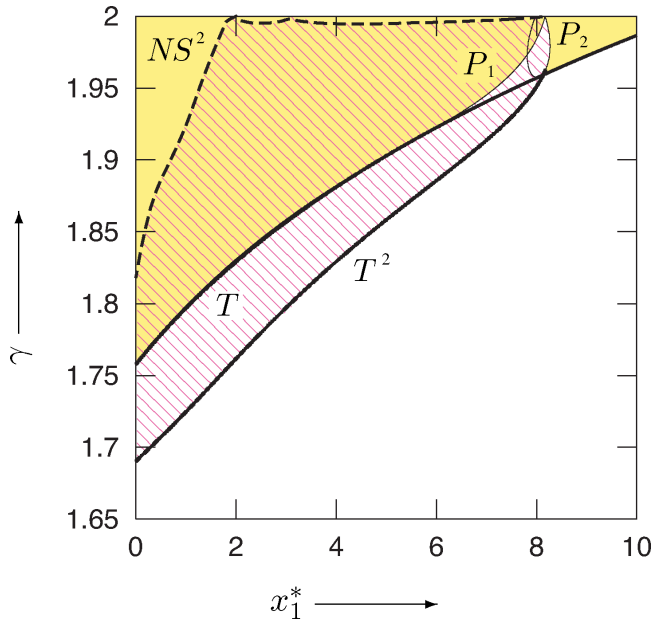

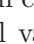

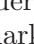


Fig. 3. Bifurcations in PMART.

several of the same sets. If  $m = 1$ , it will be omitted. The bifurcations in the entire parameter region shown in Fig. 3 are related to false images, whereas no bifurcation occurs for the stable fixed point corresponding to the true image. In the parameter regions with shading patterns  and , there is a possibility that PMART will converge to a false image, depending on the initial value of the state. The mechanism is explained below.

There is an enlarged diagram in Fig. 4. The circled point labeled  $TP$  denotes a codimension-two bifurcation [Yoshinaga & Kawakami, 1990; Kawakami & Yoshinaga, 1995], which occurs with both tangent and period-doubling bifurcations. We can observe a stable fixed point,  ${}_0PD$ , in the parameter region with pattern . When varying the value of a parameter through the period-doubling bifurcation curve,  $P_2$ , terminating at points  $a$  and  $b$ , from the inside to the outside of the shaded pattern, a two-periodic point occurs according to the following bifurcation formula:

$${}_0PD \rightarrow {}_1PI + {}_0PD^2$$

where the left and right sides of the arrow respectively indicate invariant sets before and after the bifurcation. The stable two-periodic point,  ${}_0PD^2$ , exists in shaded region , bordered by the tangent bifurcation ( $T^2$ ) and the Neimark–Sacker bifurcation ( $NS^2$ ) curves. We can see that two different false images coexist in the parameter region that is overlapped by the two shaded patterns.

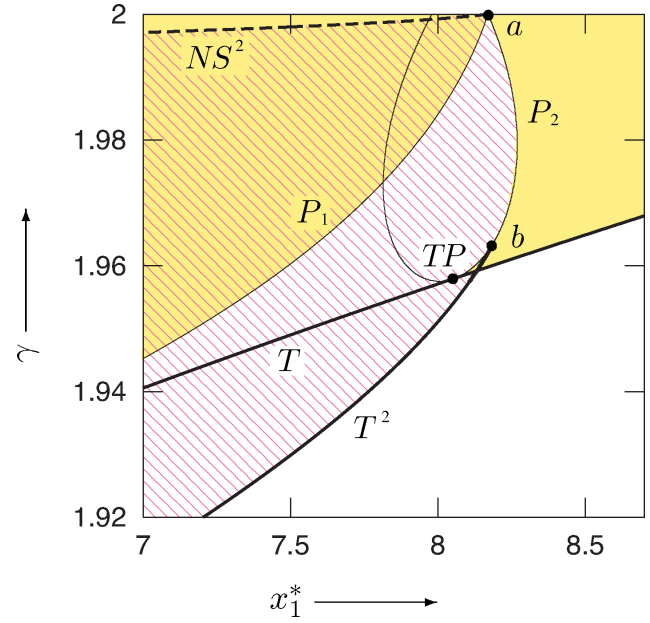
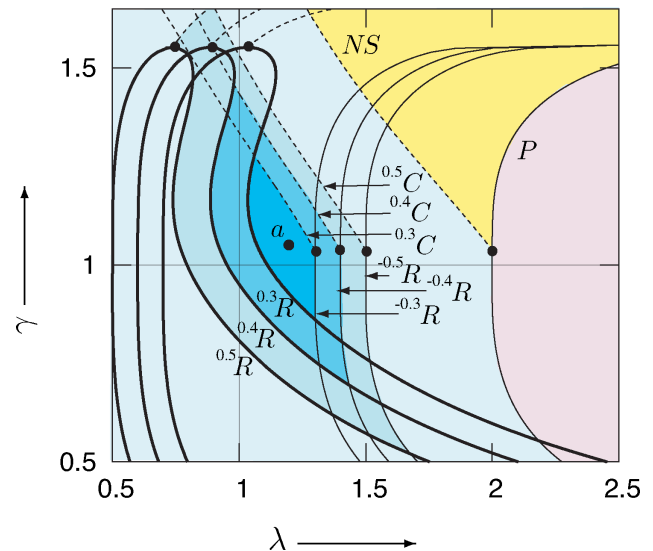





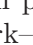

Fig. 4. An enlarged diagram of Fig. 3.

#### 4.2. Analysis of extended PMART


Figure 5 shows a phase transition diagram of fixed points observed in the extended PMART of Eq. (9) with  $J = 4$ . In the figure, the parameter sets of equal values of characteristic multipliers of fixed points are indicated by the solid and dashed curves with the symbols  $\mu^*R$  and  $\rho^*C$  for real multiplier  $\mu^*$  and the absolute value  $\rho^*$  of a complex multiplier, respectively, each of which is the maximum absolute value of all characteristic multipliers. Period-doubling and Neimark–Sacker bifurcations


 Fig. 5. Phase transition of fixed points observed in  $g$  with  $J = 4$ .

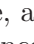

are conventionally denoted by  $P$  and  $NS$ , which are equivalent to  $^{-1}R$  and  $^1C$ , respectively.

There is a unique stable fixed point in the parameter regions without shading in the diagram, and with shading patterns , , and . In contrast, in the regions with patterns  and  surrounded by the Neimark–Sacker and period-doubling bifurcation curves, the fixed point is unstable, and a solution does not converge to the fixed point corresponding to the phantom image. By increasing the value of  $\lambda$  and keeping  $\gamma$  fixed (e.g.  $\gamma = 0.9$ ), through bifurcation curve  $P$ , the bifurcation formula is given by

$${}_0PD \rightarrow {}_1PI + {}_0PD^2.$$

However, when the parameters pass through the Neimark–Sacker bifurcation curve  $NS$  going from the outside to the inside of region , we have the following formula:

$${}_0PD \rightarrow {}_2PD + ICC.$$

The parameter curves of equal characteristic multipliers are shown for the maximum absolute values of 0.3, 0.4 and 0.5. We can see that there is a fixed point with characteristic multipliers whose maximum absolute value is less than 0.3 in the region with pattern . Therefore, a parameter in this region provides faster convergence in the neighborhood of the stable fixed point. Note that the system at parameter  $(\lambda, \gamma) = (1, 1)$ , denoted by  $+$  in the diagram, corresponds to MART, and the parameter point is located outside region . Indeed, a simulation result comparing the extended PMART at  $(\lambda, \gamma) = (1.2, 1.05)$ , indicated by the circled point with  $a$  in Fig. 5, and MART is plotted in Fig. 6,

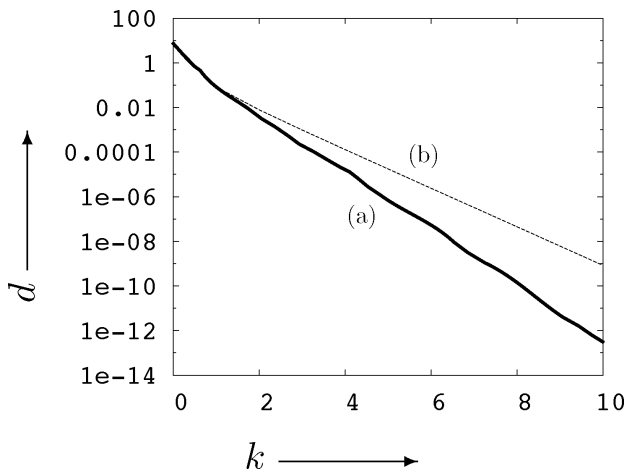


Fig. 6. The distance  $d$  for the time series of (a) the extended PMART and (b) MART for  $J = 4$ .

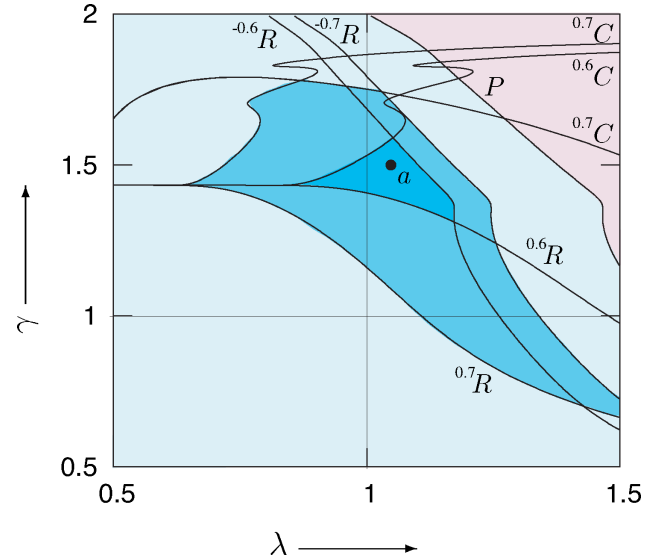



Fig. 7. Phase transition of fixed points observed in  $g$  with  $J = 25$ .

showing the root mean square distance between the reconstructed value and the fixed point, normalized by the standard deviation [Gordon & Herman, 1974], for the time series. The initial state for the iterations was set to a constant image. In the graph, lines (a) and (b) are the results using the extended PMART and MART. We can see that the proposed method leads to faster convergence, which is shown by the steep slope in log scale.

A phase transition for the second example ( $J = 25$ ) is shown in Fig. 7. Similar to the first example, we can see that parameter region , in which the maximum absolute value of the characteristic multiplier is at a minimum, does not include parameter point  $(\lambda, \gamma) = (1, 1)$ . The graph of the time series

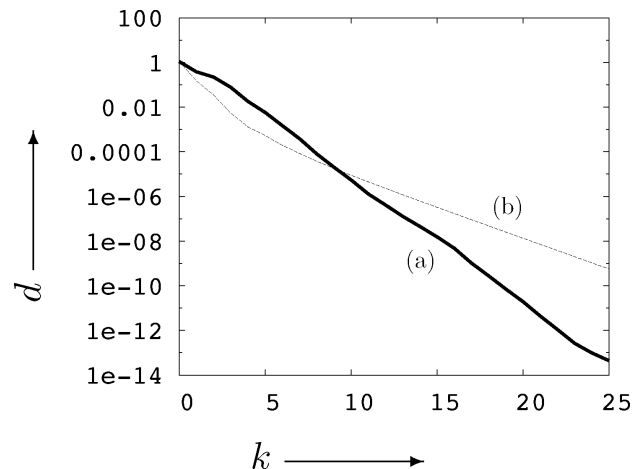


Fig. 8. The distance  $d$  for the time series of (a) the extended PMART and (b) MART for  $J = 25$ .

of the extended PMART at parameter point  $a$  in Fig. 7 or with parameter values  $(\lambda, \gamma) = (1.05, 1.5)$  and MART is also shown in Fig. 8. The extended PMART provides better results than MART after reaching the neighborhood of the fixed point.

## 5. Conclusion

We investigated an extended PMART that we proposed to accelerate convergence. The main results obtained are summarized as follows:

- (1) We calculated bifurcations of fixed and periodic points observed in PMART with multiple pixels. We conjectured that where the value of  $\gamma$  is less than and approximately equal to 2, there is a stable fixed or periodic point corresponding to a false image.
- (2) To analyze convergence speed in the neighborhood of the stable fixed point, we proposed a computational method of calculating a set of characteristic multipliers of equal value, based on the dynamical system theory. Then, through numerical experiments on systems with lower dimensions, we obtained a parameter region that gives faster convergence than the original MART.

The acceleration performance depends on the dynamical properties of the system with parameters  $\gamma$  and  $\lambda$ . We should investigate the theoretical reason as to why the parameter region in which the maximum absolute value of the characteristic multiplier is minimum, excludes value  $(\lambda, \gamma) = (1, 1)$ .

## References

- Badea, C. & Gordon, R. [2004] "Experiments with the nonlinear and chaotic behaviour of the multiplicative algebraic reconstruction technique (MART) algorithm for computed tomography," *Phys. Med. Biol.* **49**, 1455–1474.
- Byrne, C. [2004] "A unified treatment of some iterative algorithms in signal processing and image reconstruction," *Inverse Probl.* **20**, 103–120.
- Gordon, R., Bender, R. & Herman, G. [1970] "Algebraic reconstruction technique (ART) for three-dimensional electron microscopy and X-ray photography," *J. Theoret. Biol.* **29**, 471–482.
- Gordon, R. & Herman, G. [1974] "Three-dimensional reconstruction from projections: A review of algorithms," *Int. Rev. Cytol.* **38**, 111–151.
- Herman, G. & Meyer, L. [1993] "Algebraic reconstruction techniques can be made computationally efficient," *IEEE Trans. Med. Imag.* **12**, 600–609.
- Kak, A. & Slaney, M. [1987] *Principles of Computerized Tomographic Imaging* (IEEE Press, Piscataway, NJ).
- Kawakami, H. [1984] "Bifurcation of periodic responses in forced dynamic nonlinear circuits: Computation of bifurcation values of the system parameters," *IEEE Trans. Circuits Syst.* **CAS-31**, 246–260.
- Kawakami, H. & Yoshinaga, T. [1995] "Codimension two bifurcation and its computational algorithm," in *Bifurcation and Chaos: Theory and Applications*, ed. Awrejcewicz, J. (Springer-Verlag, Berlin), pp. 97–132.
- Man, B., Nuyts, J., Dupont, P., Marchal, G. & Suetens, P. [2001] "An iterative maximum-likelihood polychromatic algorithm for CT," *IEEE Trans. Med. Imag.* **20**, 999–1008.
- Mueller, K., Yagel, R. & Wheller, J. [1999] "Antialiasing three-dimensional cone-beam reconstruction of low-contrast objects with algebraic methods," *IEEE Trans. Med. Imag.* **18**, 519–537.
- Shepp, L. & Vardi, Y. [1982] "Maximum likelihood reconstruction in positron emission tomography," *IEEE Trans. Med. Imag.* **1**, 113–122.
- Snyder, D., Schulz, T. & O'Sullivan, J. [1992] "Deblurring subject to nonnegativity constraints," *IEEE Trans. Sign. Process.* **40**, 1143–1150.
- Stark, H. [1987] *Image Recovery: Theory and Application* (Academic, FL).
- Wang, G., Snyder, D., O'Sullivan, J. & Vannier, M. [1996] "Iterative deblurring for CT metal artifact reduction," *IEEE Trans. Med. Imag.* **15**, 657–664.
- Yoshinaga, T. & Kawakami, H. [1990] "Codimension two bifurcation problems in forced nonlinear circuits," *IEICE Trans. Fund. Electron. Commun. Comput. Sci.* **E-73**, 817–824.